PROCEEDINGS OF SCIENCE

Light Hadron Spectroscopy at BESIII

Jingqing Zhang[*†]
Ruhr-Universität Bochum, Germany
E-mail: jzhang@ep1.ruhr-uni-bochum.de

The BESIII experiment has collected the world's largest samples of J/ψ and $\psi(3686)$ decay events since 2009, which are ideal to study light hadron spectroscopy. Recent BESIII results in this field are presented, including the line shape of the $X(1835)$, observation of $e^+e^- \to \eta Y(2175)$ at center-of-mass energies above 3.7 GeV, partial wave analysis of $J/\psi(\psi(3686)) \to \pi^+\pi^-\eta'$ and the study of $J/\psi \to \gamma\eta\pi^0$.

XVII International Conference on Hadron Spectroscopy and Structure - Hadron2017
25-29 September, 2017
University of Salamanca, Salamanca, Spain

[*]Speaker.
[†]On behalf of BESIII Collaboration

PoS(Hadron2017)027

1. Introduction

Quantum Chromo-Dynamics (QCD) is one of the fundamental theories in modern high energy physics. Light hadron spectroscopy plays a crucial role in examining and understanding QCD theory in the non-perturbative energy region. The BESIII detector [1] located at BEPCII in Beijing has collected 1.31×10^9 J/ψ events [2] and 4.48×10^8 $\psi(3686)$ events [3, 4] since 2009. The decays of J/ψ and $\psi(3686)$ provide good chances to study light hadron spectroscopy.

2. Recent Results from BESIII

2.1 Line Shape of the $X(1835)$ in $J/\psi\to\gamma\eta'\pi^+\pi^-$

The $X(1835)$ was first observed by the BESII experiment in the $\eta'\pi^+\pi^-$ invariant mass spectrum in $J/\psi\to\gamma\eta'\pi^+\pi^-$ decays [7]. It was later confirmed by the BESIII in studies of the same process [8] and the spin-parity was determined to be $J^P=0^-$ in the partial wave analysis of $J/\psi\to\gamma\eta K^0_SK^0_S$ [9].

The line shape of the $X(1835)\to\eta'\pi^+\pi^-$ was studied with a data sample of 1.09×10^9 J/ψ events accumulated by the BESIII experiment in 2012 [5], and an abrupt in the line-shape was found near the $p\bar{p}$ mass threshold [10]. Two models were used to describe the distorted line shape near the threshold. In the first model, a Flattè formula [11] is used for the $X(1835)$ line shape. The fit result is shown in Fig. 1 and it is found that $X(1835)$ strongly couples to $p\bar{p}$ with significance larger than 7σ. The second model consists of the coherent sum of two Breit-Wigner near $p\bar{p}$ threshold: a

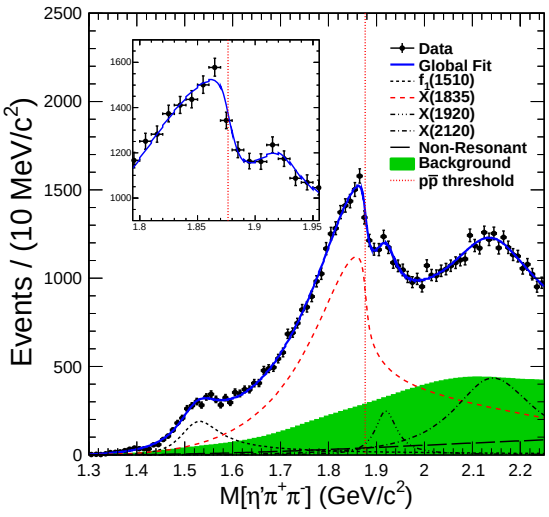

Figure 1: Fit results of using Flatté formula.

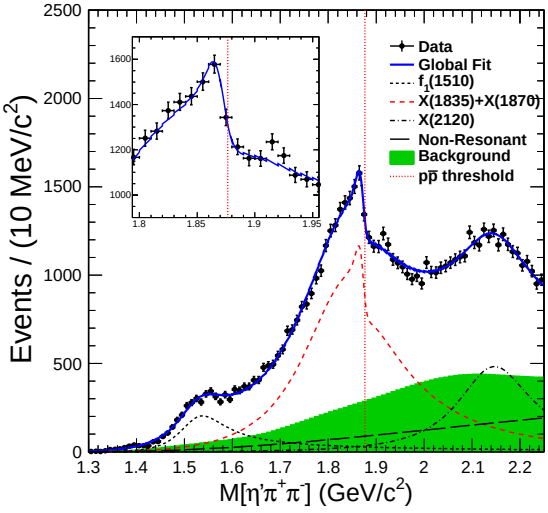

Figure 2: Fit results of using a coherent sum of two Breit-Wigner amplitudes.

narrow resonance (denoted as "$X(1870)$") and the $X(1835)$. The fit result for the second model is shown in Fig. 2. The significance of the $X(1870)$ is found to be larger than 7σ. With current data, both models fit the data well with fit qualities, and both suggest the existence of a state, either a broad state with strong couplings to $p\bar{p}$, or a narrow state just below $p\bar{p}$ mass threshold.

2.2 Observation of $e^+e^- \to \eta Y(2175)$ at center-of-mass energies above 3.7 GeV

The $Y(2175)$ was observed in the initial-state-radiation (ISR) process $e^+e^- \to \gamma_{\rm ISR}\phi f_0(980)$ [12, 13] and in J/ψ hadronic decays [14, 15]. Since the process $J/\psi \to \eta Y(2175)$ has been observed [14, 15], it is natural to expect the production of $\eta Y(2175)$ in $\psi(3686)$ decays as well as in direct e^+e^- annihilation in the non-resonant energy region.

In Ref. [16], $e^+e^- \to \eta Y(2175)$ was studied with data samples at the $\psi(3686)$ peak and at higher energies up to 4.6 GeV accumulated at BESIII [3, 4, 6]. The invariant mass distributions of $\phi f_0(980)$ for the seven data samples with $\sqrt{s} > 3.7$ GeV are shown in Fig. 3, individually. A

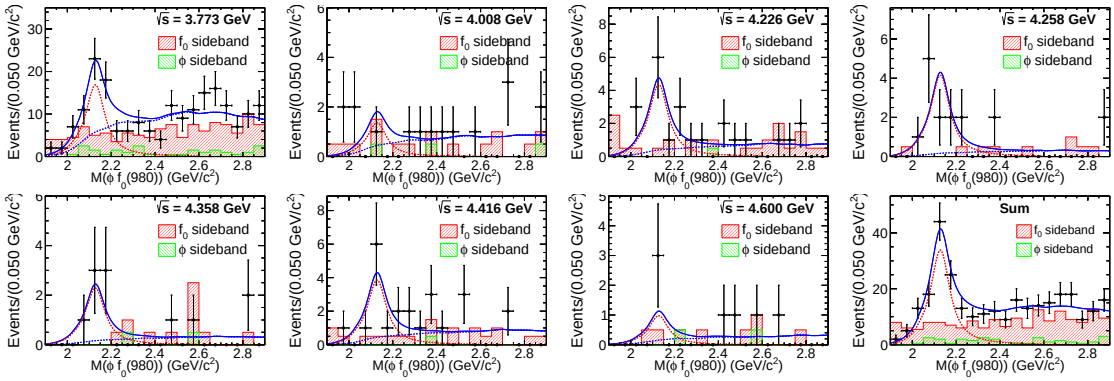

Figure 3: Invariant mass distributions of $\phi f_0(980)$ and the projections of the simultaneous fit (solid curve) at the different c.m. energies, as well as the sum of them (bottom right, marked as "Sum").

simultaneous fit is applied to all the data samples with $\sqrt{s} > 3.7$ GeV to extract the yields of signal events. Fit projections are shown in Fig. 3. The joint statistical significance of the $Y(2175)$ signal is estimated to be larger than 10σ. The signal yields, significance and Born cross section are listed in Table 1.

$\sqrt{s}$ (GeV)	$\mathscr{L}_{\rm int}$ (pb^{-1})	$N^{\rm obs}$	$\sigma^{\rm B}$ (pb)	Significance
3.686	666	19.0 ± 9.0	$1.72 \pm 0.82 \pm 1.00$	1.5σ
3.773	2917	47.4 ± 9.1	$0.93 \pm 0.18 \pm 0.15$	6.2σ
4.008	482	3.8 ± 2.6	$0.40 \pm 0.27 \pm 0.34$	1.0σ
4.226	1092	12.3 ± 4.1	$0.53 \pm 0.17 \pm 0.05$	3.8σ
4.258	826	11.6 ± 3.7	$0.65 \pm 0.21 \pm 0.08$	4.2σ
4.358	540	6.4 ± 2.7	$0.53 \pm 0.22 \pm 0.07$	2.9σ
4.416	1029	10.8 ± 4.1	$0.46 \pm 0.17 \pm 0.21$	3.2σ
4.600	567	2.7 ± 1.9	$0.20 \pm 0.14 \pm 0.02$	1.5σ

Table 1: Summary of the data samples and the cross section measurements of $e^+e^- \to \eta Y(2175) \to \eta\phi f_0(980) \to \eta\phi\pi^+\pi^-$.

The same analysis is also performed to the data at $\sqrt{s} = 3.686$ GeV. No significant $Y(2175)$ is observed and the upper limit is set to be $\mathscr{B}(\psi(3686) \to \eta Y(2175)) \cdot \mathscr{B}(Y(2175) \to \phi f_0(980) \to \phi\pi^+\pi^-) < 2.2 \times 10^{-6}$ at the 90% confidence level (C.L.) using a Bayesian approach. A search for

$e^+e^- \to \eta' Y(2175)$ is also performed to the data with $\sqrt{s} > 3.7$ GeV. No significant $Y(2175)$ or any other structure is observed. The upper limit of the $Y(2175)$ signal events is set to be 27.6 at 90% C.L. and the upper limit on the ratio of the cross section $R = \frac{\sigma_{\eta' Y(2175)}}{\sigma_{\eta Y(2175)}}$ is determined to be 0.43 at the 90% C.L. by assuming this ratio is the same at different c.m. energy points.

2.3 Partial Wave Analysis of $J/\psi(\psi(3686)) \to \pi^+\pi^-\eta'$

Using the samples of 1.31×10^9 J/ψ events and 4.48×10^8 $\psi(3686)$ events accumulated with the BESIII detector, a partial wave analysis (PWA) of the decay $J/\psi(\psi(3686)) \to \pi^+\pi^-\eta'$ is performed [17], the measured branching fractions for each components are summarized in Table 2.

Channel	$\mathscr{B}$	PDG
$J/\psi \to \rho\eta'$	$(7.90 \pm 0.19 \pm 0.49) \times 10^{-5}$	$(10.5 \pm 1.8) \times 10^{-5}$
$J/\psi \to \omega\eta'$	$(2.08 \pm 0.30 \pm 0.14) \times 10^{-4}$	$(1.82 \pm 0.21) \times 10^{-4}$
$J/\psi \to \rho(1450)\eta', \rho(1450) \to \pi^+\pi^-$	$(3.28 \pm 0.55 \pm 0.44) \times 10^{-6}$	
$J/\psi \to \pi^+\pi^-\eta'_{\rm NR}$	$(3.29 \pm 0.20 \pm 0.26) \times 10^{-5}$	
$J/\psi \to \pi^+\pi^-\eta'_{\rm (Inc)}$	$(1.36 \pm 0.02 \pm 0.08) \times 10^{-4}$	
	Solution I	
$\psi(3686) \to \rho\eta'$	$(1.02 \pm 0.11 \pm 0.24) \times 10^{-5}$	$(1.9^{+1.7}_{-1.2}) \times 10^{-5}$
$\psi(3686) \to \pi^+\pi^-\eta'_{\rm (NR)}$	$(5.13 \pm 1.23 \pm 0.64) \times 10^{-6}$	
	Solution II	
$\psi(3686) \to \rho\eta'$	$(5.69 \pm 1.28 \pm 2.36) \times 10^{-6}$	$(19.^{+17.}_{-12.}) \times 10^{-6}$
$\psi(3686) \to \pi^+\pi^-\eta'_{\rm (NR)}$	$(5.13 \pm 1.14 \pm 0.62) \times 10^{-6}$	
$\psi(3686) \to \pi^+\pi^-\eta'_{\rm (Inc)}$	$(1.51 \pm 0.14 \pm 0.23) \times 10^{-5}$	

Table 2: The the measured branching fractions.

In the decay $J/\psi \to \pi^+\pi^-\eta'$, the basic fit solution is found to contain four components, namely the ρ, ω, $\rho(1450)$ intermediate states as well as the non-resonant (NR) contribution. In the decay $\psi(3686) \to \pi^+\pi^-\eta'$, the basic solution includes a ρ component interfering with NR component due to the low statistics, and two solutions with the same fit quality are found, corresponding to the case of destructive and constructive interference between the two components with a relative phase angle $(120.3 \pm 16.6)^\circ$ and $(45.6 \pm 17.5)^\circ$, respectively. The fit results for J/ψ and $\psi(3686)$ decays are shown in Fig. 4 and 5, respectively.

With the measured branching fractions, the ratio of the branching fractions between $\psi(3686)$ and J/ψ decays to $\rho\eta'$ is calculated and listed in Table 3. These do not obviously violate the "12%" rule within one standard deviation.

2.4 Observation of $J/\psi \to \gamma\eta\pi^0$

Using a sample of $(223.7 \pm 1.4) \times 10^6$ J/ψ events collected by the BESIII detector [2], the decay $J/\psi \to \gamma\eta\pi^0$ was studied [18]. The branching fraction is measured to be $\mathscr{B}(J/\psi \to \gamma\eta\pi^0) = (2.14 \pm 0.18(\text{stat.}) \pm 0.25(\text{syst.})) \times 10^{-5}$. To investigate the intermediate resonant process $J/\psi \to$

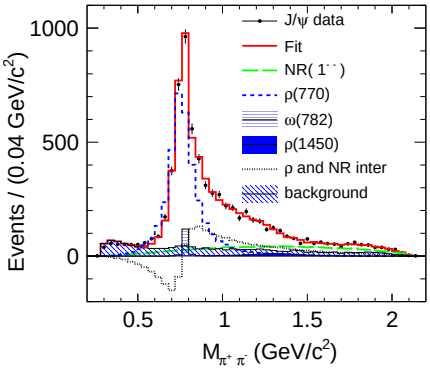

Figure 4: Comparisons of the distributions of $M_{\pi^+\pi^-}$ between data and PWA fit projections for the decay $J/\psi \to \pi^+\pi^-\eta'$.

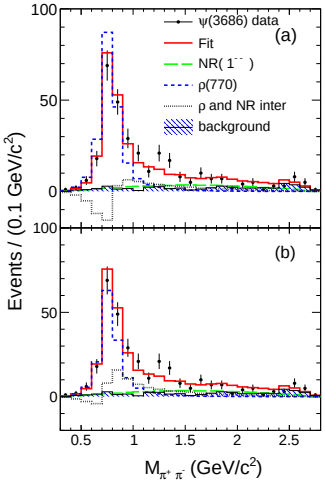

Figure 5: Comparisons of the distributions of $M_{\pi^+\pi^-}$ between data and PWA fit projections for the decay $\psi(3686) \to \pi^+\pi^-\eta'$ with (a) destructive and (b) constructive interferences.

	Solution I	Solution II
$\frac{\mathcal{B}(\psi(3686)\to\pi^+\pi^-\eta')_{(\mathrm{NR})}}{\mathcal{B}(J/\psi\to\pi^+\pi^-\eta')_{(\mathrm{NR})}}$	$15.6\pm3.9\pm2.3$	$15.6\pm3.6\pm2.3$
$\frac{\mathcal{B}(\psi(3686)\to\rho\eta')}{\mathcal{B}(J/\psi\to\rho\eta')}$	$12.9\pm1.4\pm3.1$	$7.2\pm1.6\pm3.0$
$\frac{\mathcal{B}(\psi(3686)\to\pi^+\pi^-\eta')_{(\mathrm{Inc})}}{\mathcal{B}(J/\psi\to\pi^+\pi^-\eta')_{(\mathrm{Inc})}}$	$11.1\pm1.0\pm1.8$	

Table 3: The ratios of branching fractions between $\psi(3686)$ and J/ψ decay to $\rho\eta'$, NR and inclusive decays (%). The first uncertainties are statistical and the second systematic.

$\gamma a_0(980)(a_2(1320)) \to \gamma\eta\pi^0$, a fit to the $\eta\pi^0$ mass spectrum is performed, which is shown in Fig. 6. In this fit, the signal shape for $a_0(980)$ is a Flattè formula and for $a_2(1320)$ is a Breit-Wigner function. The statistical significance is only 0.5σ for $a_0(980)$ and 2.9σ for $a_2(1320)$. Therefore, upper limits on the branching fractions are set to be $\mathcal{B}(J/\psi \to \gamma a_0(980) \to \gamma\eta\pi^0) < 2.5\times10^{-6}$ and $\mathcal{B}(J/\psi \to \gamma a_2(1320) \to \gamma\eta\pi^0) < 6.6\times10^{-6}$ at the 95% C.L..

References

[1] M. Ablikim *et al.*, (BESIII Collaboration), Nucl. Instrum. Meth. A **614**, 345 (2010).

[2] M. Ablikim *et al.* (BESIII Collaboration), Chin. Phys. C **41**, 013001 (2017).

[3] M. Ablikim *et al.* (BESIII Collaboration), Chin. Phys. C **37**, 063001 (2013).

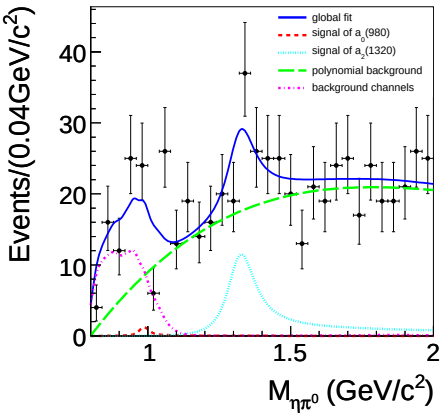

Figure 6: Fit to $\eta\pi^0$ invariant mass distribution.

[4] M. Ablikim *et al.* (BESIII Collaboration), arXiv:1709.03653.

[5] M. Ablikim *et al.* (BESIII Collaboration), Chin. Phys. C **36**, 915 (2012).

[6] M. Ablikim *et al.* (BESIII Collaboration), Chin. Phys. C **39**, 093001 (2015).

[7] M. Ablikim *et al.* (BES Collaboration), Phys. Rev. Lett. **95**, 262001 (2005).

[8] M. Ablikim *et al.* (BESIII Collaboration), Phys. Rev. Lett. **106**, 072002 (2011).

[9] M. Ablikim *et al.* (BESIII Collaboration), Phys. Rev. Lett. **115**, 091803 (2015).

[10] M. Ablikim *et al.* (BESIII Collaboration), Phys. Rev. Lett. **117**, 042002 (2016).

[11] S. M. Flatté, Phys. Lett. B **63**, 224 (1976).

[12] B. Aubert *et al.* (BABAR Collaboration), Phys. Rev. D **74**, 091103(R) (2006);

[13] C. P. Shen *et al.* (Belle Collaboration), Phys. Rev. D **80**, 031101(R) (2009).

[14] M. Ablikim *et al.* (BES Collaboration), Phys. Rev. Lett. **100**, 102003 (2008).

[15] M. Ablikim *et al.* (BESIII Collaboration), Phys. Rev. D **91**, 052017 (2015).

[16] M. Ablikim *et al.* (BESIII Collaboration), Phys. Rev. D **96**, 012001 (2017).

[17] M. Ablikim *et al.* (BESIII Collaboration), arXiv:1709.00018.

[18] M. Ablikim *et al.* (BESIII Collaboration), Phys. Rev. D **94**, 072005 (2016).

PoS(Hadron2017)027